

**REMARKS**

Reconsideration and withdrawal of the rejections set forth in the Office Action are respectfully requested in view of this amendment and the following reasons. By this amendment, claims 2, 9, 17, 24-28, 30, 58, 60, 69, and 70 have been amended, and claims 10-13, 16, 18, 31-57, 61-66, 68, 71, and 72 have been canceled. The cancellation of claims 10-13, 16, 18, 31-57, 61-66, 68, 71, and 72, previously withdrawn from consideration is made without prejudice or disclaimer to the subject matter contained therein. Accordingly, claims 1-9, 14, 15, 17, 19-30, 58-60, 67, 69, and 70 are pending in this application.

Claims 2, 9, 17, 24-28, 30, 58, 60, 69, and 70 have been amended to correct informalities and/or to more clearly define the present subject matter. Thus, it is respectfully submitted that the above amendments introduce no new matter within the meaning of 35 U.S.C. §132. For at least these reasons, entry of the present Amendment is therefore respectfully requested. Accordingly, Applicants request reconsideration and timely withdrawal of the pending rejections for the reasons discussed below.

***Information Disclosure Statement***

The Office Action states that “[t]he information statement filed 9-26-2006 fails to comply with 37 CFR 1.98(a)(2), which requires a legal copy of each cited foreign patent document; each non-patent literature publication or that portion which caused it to be listed; and all other information or that portion which caused it to be listed. It has been placed in the application file, but the information referred to therein has not been considered. No copy of NPL to D. Sabourdy

et al has been received and has been crossed in the IDS.”

In response to the above, Applicants have attached hereto a copy of the above-indicated document. Accordingly, Applicants respectfully request the Examiner to consider the information referred to therein.

***Claim Objection***

1. Claim 58 was objected to because of the following informalities: depends from claim 15(b) and should read claim 15.
2. Claim 60 was objected to because of the following informalities: depends from claim 15(b) and should read claim 15.
3. Claim 69 was objected to because of the following informalities: applicant’s terms of “for use” is considered intended use.
4. Claim 69 was objected to because of the following informalities: the use of “so on” is not considered legal phraseology.
5. Claim 70 was objected to because of the following informalities: applicant’s terms of “for use” is considered intended use.
6. Claim 70 was objected to because of the following informalities: the use of “vice versa” is not considered legal phraseology.

In response to the first and second reasons for objection, claims 58 and 60 have been amended to make proper reference to -- claim 15 -- from “claim 15(b),” as shown above.

In response to the third and fourth reasons for objection, claim 69 has been amended to

delete the terms “for use” and “so on,” as shown above.

In response to the fifth and sixth reasons for objection, claim 70 has been amended to delete the terms “for use” and “vice versa,” as shown above.

Applicants respectfully submit that claims 58, 60, 69, and 70, as amended, overcome the stated objection. Accordingly, Applicants respectfully request withdrawal of the objection to claims 58, 60, 69, and 70.

***Rejections Under 35 U.S.C. §112***

Claims 2, 9, 24-28, 30, 69, and 70 stand rejected under 35 U.S.C. §112, second paragraph, as being allegedly indefinite for failing to particularly point out and distinctly claim the subject matter which applicant regards as the invention.

1. Claim 2 recites the limitation “said single gain medium” in line 2. There is insufficient antecedent basis for this limitation in the claim.
2. Claim 9 recites the limitation “the output end reflector” in line 1. There is insufficient antecedent basis for this limitation in the claim.
3. Claim 24 recites the limitation “the front facet” in line 1. There is insufficient antecedent basis for this limitation in the claim.
4. Claim 24 recites the limitation “the first light channel” in line 5. There is insufficient antecedent basis for this limitation in the claim.
5. Claim 24 recites the limitation “the rear facet” in line 7. There is insufficient antecedent basis for this limitation in the claim.

6. Claim 25 recites the limitation “the output end” in line 1. There is insufficient antecedent basis for this limitation in the claim.
7. Claim 26 recites the limitation “the single output” in line 2. There is insufficient antecedent basis for this limitation in the claim.
8. Claim 27 recites the limitation “the output end” in line 2. There is insufficient antecedent basis for this limitation in the claim.
9. Claim 27 recites the limitation “the front [facet]” in line 3. There is insufficient antecedent basis for this limitation in the claim.
10. Claim 27 recites the limitation “the first light channel” in line 8. There is insufficient antecedent basis for this limitation in the claim.
11. Claim 28 recites the limitation “the substantially transmitting regions” in line 1. There is insufficient antecedent basis for this limitation in the claim.
12. Claim 30 recites the limitation “the front facet” in line 1. There is insufficient antecedent basis for this limitation in the claim.
13. Claim 30 recites the limitation “the single beam splitting sub-region” in line 2. There is insufficient antecedent basis for this limitation in the claim.
14. Claim 69 recites the limitation “the first light channel” in line 9. There is insufficient antecedent basis for this limitation in the claim.
15. Claim 70 requires for the light to be reflected, however the regions are recited as having “transmission or reflectivities,” thereby the claim is allegedly ambiguous.

In response to the first reason for rejection, claim 2 has been amended to replace the term

“the single gain medium,” recited in line 2, with -- a single gain medium --.

In response to the second reason for rejection, claim 9 has been amended to replace the term “the output end reflector,” recited in line 1, with -- an output end reflector --.

In response to the third through fifth reasons for rejection, claim 24 has been amended to make proper reference to claim 22, rather than to claim 21, and replace the term “the first light channel,” recited in line 5, with -- a first light channel --. It is noted that claim 22, upon which claim 24 depends, recites “front and rear facets” in line 2 and thus provides sufficient antecedent basis.

In response to the sixth reason for rejection, claim 25 has been amended to replace the term “the output end,” recited in line 1, with -- an output end --.

In response to the seventh reason for rejection, claim 26 has been amended to replace the term “the single output,” recited in line 2, with -- a single output --.

In response to the eighth through tenth reasons for rejection, claim 27 has been amended to make proper reference to claim 22, rather than to claim 21, and replace the terms “the output end” and “the first light channel,” respectively recited in lines 2 and 8, with -- an output end -- and -- a first light channel --, respectively. It is noted that claim 22, upon which claim 27 depends, recites “front and rear facets” in line 2 and thus provides sufficient antecedent basis.

In response to the eleventh reason for rejection, claim 28 has been amended to proper reference to claim 27, rather than to claim 21. It is noted that claim 27, upon which claim 28 depends, recites “substantially light transmitting regions” in line 7 and thus provides sufficient antecedent basis.

In response to the twelfth and thirteenth reasons for rejection, claim 30 has been amended to make proper reference to claim 22, rather than to claim 21, and replace the term "the single beam splitting sub-region," recited in line 2, with -- a single beam splitting sub-region --. It is noted that claim 22, upon which claim 30 depends, recites "front and rear facets" in line 2 and thus provides sufficient antecedent basis.

In response to the fourteenth reason for rejection, claim 69 has been amended to replace the term "the first light channel," recited in line 9, with -- a first light channel --.

In response to the fifteenth reason for rejection, claim 70 has been amended to replace the term "transmission or reflectivities," recited in line 5, with -- transmission and reflectivity --. However, it is submitted that the regions recited as having "transmission or reflectivities" are **the front and rear facets** and the light is reflected from the rear facet. The claim recites that "*the front facet includes a substantially transmitting region and at least one predetermined beam splitting region; and the rear facet includes at least one predetermined beam splitting region [...] such that light **is reflected from the beam splitting region of the rear facet** towards the beam splitting region of the front facet*" (Emphasis added). Although Applicants consider that the above definition is clear with regard to the configuration and operation of the beam coupler element, Applicants have slightly amended the claim wording which makes the definition even more clear.

In view of the above, Applicants respectfully request withdrawal of the 35 U.S.C. §112, second paragraph, rejection of claims 2, 9, 24-28, 30, 69, and 70.

***Allowable Subject Matter***

Applicants appreciate the Examiner's indication that claims 1-9, 14, 15, 17, 19-30, 58-60, 67, 69, and 70 contain allowable subject matter. Claims 2, 9, 24-28, 30, 58, 60, 69, and 70 have been amended to overcome the claim objections and/or 35 U.S.C. §112, second paragraph rejections above. Accordingly, Applicants submits that claims 2, 9, 24-28, 30, 58, 60, 69, and 70 are in condition for allowance.

**CONCLUSION**

Applicants believe that a full and complete response has been made to the pending Office Action and respectfully submit that all of the stated objections and grounds for rejection have been overcome or rendered moot. Accordingly, Applicants respectfully submit that all pending claims are allowable and that the application is in condition for allowance.

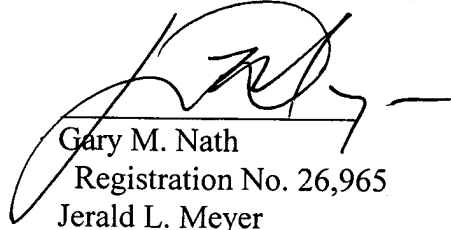
Should the Examiner feel that there are any issues outstanding after consideration of this response, the Examiner is invited to contact Applicants' undersigned representative at the number below to expedite prosecution.

Prompt and favorable consideration of this Reply is respectfully requested.

January 12, 2009

THE NATH LAW GROUP  
112 South West Street  
Alexandria, VA 22314-2891  
Tel: 703-548-6284  
Fax: 703-683-8396

Respectfully submitted,  
**THE NATH LAW GROUP**



Gary M. Nath  
Registration No. 26,965  
Jerald L. Meyer  
Registration No. 41,194  
Sung Yeop Chung  
Ltd. Rec. No. L0449  
Customer No. 20529



u

# Efficient coherent combining of widely tunable fiber lasers

David Sabourdy, Vincent Kermène, Agnès Desfarges-Berthelebot, Laurent Lefort and  
Alain Barthélémy

IRCOM, UMR CNRS 6615, 123 Av. A. Thomas, 87060 Limoges Cedex, France  
[kermene@ircom.unilim.fr](mailto:kermene@ircom.unilim.fr)

P. Even and D. Pureur

Highwave Optical Technologies, 11 rue Louis de Broglie, 22300 Lannion, France

**Abstract:** We have experimentally demonstrated coherent combining of 2 and then 4 fiber lasers, with respectively 99% and 95% combining efficiency. The combining method investigated here is based on a multi-arm resonator of interferometric configuration. In spite of its interferometric nature, the multi-arm laser operates without significant power fluctuations, even in an unprotected environment. This occurs when the arm length difference is large enough to introduce spectral modulations of period smaller than the laser bandwidth. We have also experimentally shown that the combining method is compatible with wavelength tuning. A Mach-Zehnder Fiber Laser was tuned over a wide spectral range of 60nm. Theoretically then, we confirm that the combining method can be scaled to a large number of lasers without decreasing the combining efficiency.

©2003 Optical Society of America

OCIS codes: (060.2320) Fiber optics amplifiers and oscillators; 140.3410 Laser resonators

## References and links

1. D. Sabourdy, V. Kermène, A. Desfarges-Berthelebot, L. Lefort, A. Barthélémy, C. Mahodaux and D. Pureur, "Power scaling of fibre lasers with all-fibre interferometric cavity," *Elect. Lett.* **38**, 692-693 (2002).
2. A. Shirakawa, T. Saitou, T. Sekiguchi, and K. Ueda, "Coherent addition of fiber lasers by use of a fiber coupler," *Opt. Express* **10**, 1167-1172, (2002), <http://www.opticsexpress.org/abstract.cfm?URI=OPEX-10-21-1167>
3. T. B. Simpson, A. Gavrielides and P. Peterson, "Extraction characteristics of a dual fiber compound cavity," *Opt. Express* **10**, 1060-1073, (2002), <http://www.opticsexpress.org/abstract.cfm?URI=OPEX-10-20-1060>
4. P.W. Smith, "Mode selection in lasers," *Proc. IEEE* **60**, 422-440, (1972).
5. E. Desurvire, D. Bayart, B. Desthieux, S. Bigo, *Erbium-Doped Fiber Amplifiers* (Wiley, New York, 2002), chap. 4.
6. W.H. Loh, B.N. Samson, L. Dong, G.J. Cowle, K. Hsu, "High Performance Single Frequency Fiber Grating-Based Erbium-Ytterbium-Codoped Fiber Lasers," *J. Lightwave Technol.* **16**, 114, (1998).
7. P. Mollier, V. Armbruster, H. Porte, J.P. Goedgebuer, "Electrically tunable Nd<sup>3+</sup>-doped fibre laser using nematic liquid crystals," *Elect. Lett.* **31**, 1248-1250, (1995).
8. M. Auerbach, D. Wandt, C. Fallnich, H. Welling, S. Unger, "High-power tunable narrow line width ytterbium-doped double-clad fiber laser," *Opt. Commun.* **195**, 437-441, (2001).
9. C. Pedersen, T. Skettrup, "Laser modes and threshold conditions in N-mirror resonators," *J. Opt. Soc. Am. B* **13**, 926-937, (1996).
10. C. Pedersen, T. Skettrup, "Signal-flow graphs in coupled laser resonator analysis," *J. Opt. Soc. Am. A* **14**, 1791-1798, (1997).

## 1. Introduction

High efficiency coherent combining of two fiber lasers has recently been demonstrated [1-2]. The combining method is based on the use of a multi-arm resonator in an interferometric configuration. Michelson and Mach-Zehnder type resonators have been successfully used to

reach nearly 100% combining efficiency with two fiber lasers. Coupling is obtained when the two amplifying fibers share a common output mirror located on one port of a standard 50/50 coupler which mixes the two optical fields. The resonant frequencies of the circulating fields in this active interferometer self-adjust so that the intensity in the common arm of the device is maximum. This concept, which is adapted to the use of double clad doped fibers [3], brings some novel perspectives for scaling the output power of the monomode fiber lasers. In this paper we investigate the specifics of the coherent coupling in this new kind of laser resonator. We first give the condition to ensure a stable output power operation in spite of the interferometric laser design. We then show that our coherent combining method is also compatible with the broadband tuning of the laser wavelength. Finally, we discuss the number of fiber lasers that it is possible to combine.

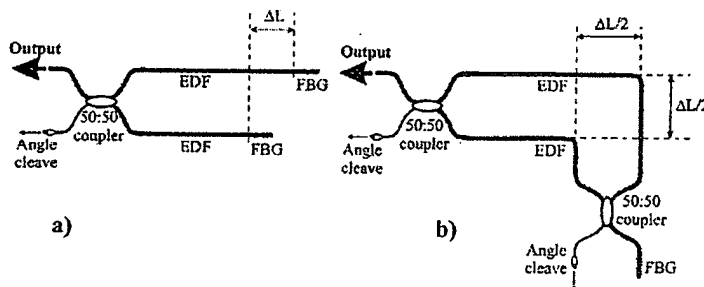


Fig. 1. Interferometric resonator configurations used for power combining: a) Michelson Fiber Laser (MFL). b) Mach-Zehnder Fiber Laser (MZFL). EDF: Erbium Doped Fiber; FBG: Fiber Bragg Grating.

The principle of our coherent combining method is based both on the self-organization property of lasers ensuring operation on modes of lowest losses [4], and on the use of an interferometric resonator configuration. A typical cavity, the Michelson laser, depicted in Fig. 1(a), is built up around a standard 50/50 coupler with each output port connected to an amplifier fiber ended by a high reflectivity mirror. Only one input port ensures light feedback towards the amplifiers with a small reflectivity achieved with a fiber cleave to make up a "3-mirror" laser. The fields from the two amplifiers are coherently coupled by interfering on the coupler. Any spurious feedback from the opposite port of the coupler into the Michelson laser must be avoided by cleaving the fiber at an angle. In that way, only the resonant frequencies with minimum losses in the shared arm (input port of the coupler with normal cleave), are amplified. Therefore, the laser spontaneously oscillates on the gain peaks which correspond to the coherent combining. The reflectivity transfer function in intensity of such an interferometer without gain is well-known and is described by:  $R(\omega) = \sin^2(\omega \Delta L / c)$  where  $\Delta L$  denotes the difference in effective length between the two arms ( $\Delta L = L_2 - L_1$ ; see Fig. 1(a)). Assuming an equal gain on each arm of the interferometer, the net gain profile provided by the set-up is modulated by  $R(\omega)$  with a maximum modulation depth. The interferometer resonator acts as a spectral periodic filter of period  $\Delta\nu = c/(2\Delta L)$ . It is also possible to achieve laser combining from a Mach-Zehnder type resonator, shown in Fig. 1(b) [1]. Both configurations, (the Mach-Zehnder fiber laser (MZFL) and the Michelson fiber laser (MFL)) operate in the same manner and they have the same features. Nevertheless, the Mach-Zehnder configuration induces a spectral filtering with a periodicity of  $\Delta\nu = c/\Delta L$  which is twice as broad than the one obtained with the Michelson configuration (see Fig. 1(b)). The advantage of this configuration consists in the use of a single fiber Bragg grating as a cavity rear mirror. The coherent combining occurs here on both sides of the interferometer. In this paper, we study

only the Mach-Zehnder fiber laser and consider both configurations to have identical behaviors.

## 2. Combining efficiency

Our experimental device, shown in Fig. 2, consists of two independent Erbium doped fiber amplifiers which are core pumped by two pigtailed laser diodes emitting at 980nm with a power up to 100mW. The Er-fibers (EDF) had lengths of ~17m corresponding to almost complete pump absorption. The two arms of the active interferometer were spliced to two 50/50 couplers. One of the output ports of the back coupler (C2) is spliced to a chirped fiber Bragg gratings (CFBG) with high reflectivity ( $\geq 98\%$ ) at 1550nm and 2nm bandwidth. The other output port is angle cleave to avoid light feedback in the cavity. The output coupler of the MZFL has a 4% reflectivity by cleaving the fiber of one input port of the other 50/50 coupler (C1). The second input port of the coupler was angle cleaved to avoid any reflection. We control the interferometer path length difference with a mechanical delay line (DL).

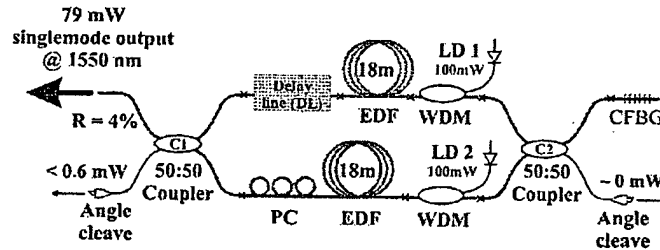


Fig. 2. Experimental set-up of the Mach-Zehnder Fiber Laser (MZFL). LD1, LD2: 980nm Pump laser diodes; EDF: Erbium doped fiber; CFBG: Chirped fiber Bragg grating @ 1550nm; WDM: Wavelength-division multiplexer; PC: Polarization controller.

We first measured the conversion efficiency of the MZFL, and then compared the performances obtained with the MZFL with those obtained with an individual fiber laser (IFL). IFL is based on the components forming one branch of the MZFL. Figure 3 shows that the MZFL threshold (Thr) of 20mW was twice the MZFL one. This is due to the fact that in each arm of the MZFL, the population inversion occurred at the same pumping level than in the IFL. The MZFL and the IFL had almost the same slope efficiency ( $\eta_L$ ) of 44%. This means that the combining efficiency was maximum, and was confirmed by the very low power leakage measured on the angle cleave outputs (Fig. 2). For the highest pumping level of  $2 \times 100\text{mW}$ , the MZFL delivered  $P_{\text{out}} = 79\text{mW}$ , almost twice the output power of an IFL (40mW). In that case, the leakage power  $P_{\text{leak}}$  is lower than a milliwatt which corresponds to a combining efficiency  $\eta = P_{\text{out}}/(P_{\text{out}} + P_{\text{leak}}) \approx 99\%$ . The laser output was not polarized, indicating that in the coupler, the two polarization states from each fiber arm were independently combined. The combining efficiency is not very sensitive to the intensity imbalance. This can be explained by a purely linear analysis, considering the interference contrast in each 50/50 coupler. In that way, the output power is  $P_{\text{out}} = (P_1 + P_2 + 2(P_1 P_2)^{1/2})/2$  when the leakage power is  $P_{\text{leak}} = (P_1 + P_2 - 2(P_1 P_2)^{1/2})/2$ ;  $P_i$  is the emitted power of the individual fiber laser  $i$ , equivalent to that forming the laser arm  $i$ . By fixing  $P_1$  to its maximum value and  $P_2 = K \cdot P_1$ ,  $K$  varying from 0 to 1, one can rewrite  $P_{\text{out}}$  and  $P_{\text{leak}}$  as:  $P_{\text{out}} = P_1(1 + K + 2(K)^{1/2})/2$ ;  $P_{\text{leak}} = P_1(1 + K - 2(K)^{1/2})/2$ . We define the combining efficiency as  $\eta = P_{\text{out}}/(P_{\text{out}} + P_{\text{leak}}) = 1/2 + K/2 + (K)^{1/2}/(1 + K)$ . Figure 4 shows theoretical and experimental variations of the combining efficiency as a function of the  $K$  factor. Experimentally, we fix  $P_1$  at its maximum value (maximum pumping) when  $P_2$  varies. One can note that individual laser combining is not greatly dependent upon power imbalance; even a 50% difference decreases the combining efficiency by only 3%.

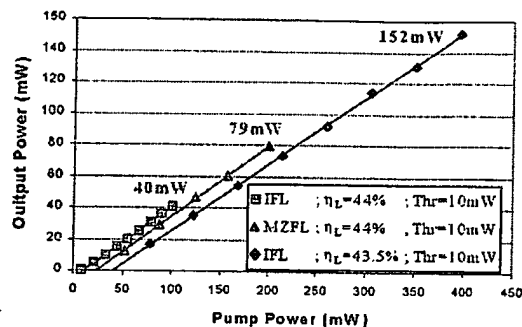


Fig. 3. Power characteristics of the different fiber laser configurations: the individual fiber laser (IFL), the Mach-Zehnder fiber laser (MZFL), the 4-arm fiber laser (4AFL) ; Thr: threshold ;  $\eta_L$ : slope efficiency.

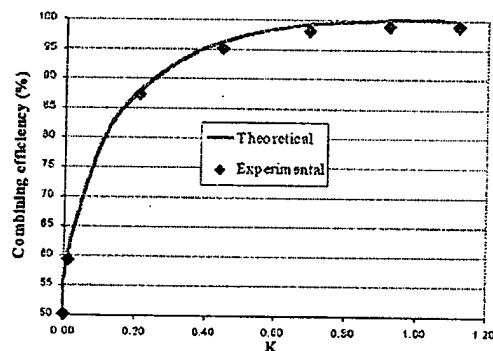


Fig. 4. Theoretical and experimental MZFL combining efficiency versus the power ratio ( $K=P_2/P_1$ ) in the two arms.

### 3. Spectral behavior of the Mach-Zehnder fiber laser

We measured the MZFL spectrum with an Anritsu optical spectrum analyzer (MS9710B) of 0.07nm spectral resolution. Experimentally, we observe some spectrum modulations which correspond to the spectral filtering of period  $\Delta\nu = c/\Delta L$ . However, the large homogeneous linewidth of Erbium doped fiber at room temperature prevents simultaneous oscillations of closely spaced wavelengths [5]. Thus, the path length difference  $\Delta L$  must be large enough to get several modulation periods  $\Delta\nu$  in a bandwidth as small as 0.3nm.

Figures 5(a), 5(b) and 5(c) show the measured spectra where  $\Delta L$  is respectively 27, 20.3 and 12.2mm. Smaller  $\Delta L$  leads to a laser spectrum with one or two groups of resonant frequencies, as shown in Figs. 5(c), 5(d) and 5(e). We also observed that the MZFL spectrum bandwidth broadens when  $\Delta L$  is decreased so that at least one resonant frequency group is always emitted. The laser gain bandwidth boundaries are given by the chirp fiber Bragg grating characteristics (2nm bandwidth at 1550nm). The MZFL resonant frequencies randomly shift inside the bandwidth due to the external perturbations which slightly change the interferometer path length difference. The condition for shifting a maximum spectrum

modulation towards its neighbor is the following:  $v \cdot [(\Delta L + \delta l)/c] - v \cdot (\Delta L/c) = 1$  i.e.  $\delta l = \lambda$ . This small value is easily reachable in non protected environment taking into account the long lengths of the interferometer arms ( $\sim 20$ m). This phenomenon is critical when the spectrum modulation period  $\Delta v$  is of the same order or larger than the laser gain bandwidth. The fluctuations of the laser output power then increase rapidly as  $\Delta L$  tends to zero.

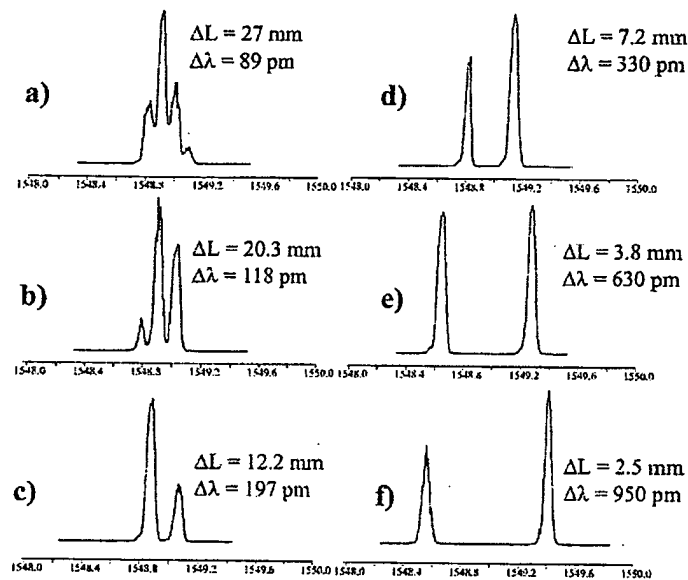


Fig. 5. Spectra of the MZFL obtained with different arm length detuning  $\Delta L$ .

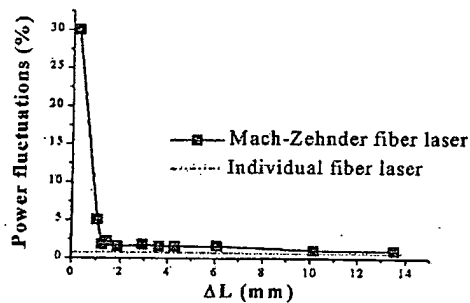


Fig. 6. Power fluctuations of the MZFL versus the path length difference  $\Delta L$  compared with those of an Individual Fiber Laser (IFL).

Figure 6 shows the evolution of power fluctuations obtained with the MZFL versus the optical path difference  $\Delta L$  by comparison with that of a standard individual fiber laser (Fabry Perot cavity). Power fluctuations have been measured during one second with a fast InGaAs photodiode of 1GHz bandwidth. Output power fluctuations are significant when  $\Delta L$  is lower

than 2mm which corresponds to a spectrum modulation period  $\Delta\lambda = 1.2\text{nm}$  to be compared to the 2nm of the Bragg grating bandwidth.

Nevertheless, and despite the MZFL being based on an interferometric architecture, it operates without any output power instabilities if the two arms of the active interferometer have a sufficiently high difference in length (Fig. 6).

#### 4. Coherent combining of widely tunable laser sources

The broad emission bandwidth of rare-earth doped fiber allows the achievement of widely tunable laser sources. In the past, many tunable fiber laser systems have been experimented either using fiber Bragg gratings [6], liquid crystals [7] or diffraction grating as dispersive elements [8]. However, the output power obtained was only a few milliwatts. The coherent combining method used in the MZFL leads to a spectrum modulation  $\Delta\nu = c/\Delta L$  which is not dependent on the laser wavelength. So, we have experimentally demonstrated that power scaling of all-fiber laser is compatible with wavelength tuning in the interferometric fiber laser.

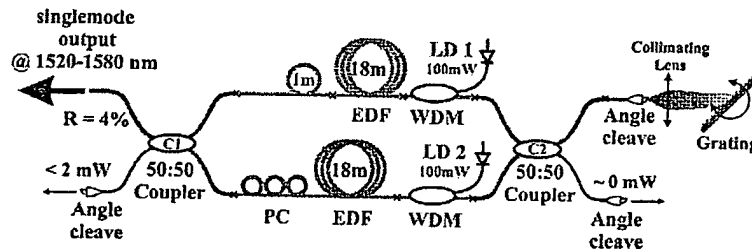


Fig. 7. Experimental set-up of the tunable Mach-Zehnder fiber laser; LD1, LD2: 980nm Pump laser diodes; EDF: Erbium doped fiber; WDM: Wavelength-division multiplexer; PC: Polarization controller.

Figure 7 depicts the experimental set-up which is used to investigate the MZFL tuning characteristics. The device is based on the Mach-Zehnder-type configuration described previously (figure 2). The two input ports of the coupler  $C_2$  were now angle cleaved. The output beam from one of them was collimated (lens of 11mm focal length) and was then sent onto a diffraction grating operating at the Littrow angle. The MZFL wavelength tuning was achieved by rotation of the grating. The diffraction grating had 830 gr/mm with a gold coating. The diffraction efficiency of the grating was close to 90% for p polarization and only 35% for the s polarization. Therefore, the diffraction grating acted as a polarizer and the radiation emitted by the MZFL was strongly linearly polarized with an extinction ratio of 50:1. Combining efficiency and intracavity losses were optimized thanks to the polarization controller (PC) in connection with the grating. The MZFL is tunable on a wide spectral range of 60nm from 1520nm to 1580nm which matches the whole gain bandwidth of the erbium doped fiber. Figure 8 shows different emission spectra obtained by rotating the diffraction grating. A maximum output power of 63mW at 1550nm was reached with a total leakage power lower than 2mW measured at the output of the angle cleaved fibers. It has to be noted that the fibers used in the MZFL had a low intrinsic birefringence with a beat length of  $\sim 1\text{m}$ . The orientation of the output beam polarization only rotates by a few degrees when the laser wavelength was tuned over the complete gain bandwidth. The combining efficiency optimized by adjusting the polarization controller at a given emission wavelength does not require additional adjustments at other wavelengths. Experimental results show a very small output power difference between the results obtained by optimizing the polarization controller at each wavelength in comparison with those obtained by only optimizing the PC at 1550nm (Fig. 9, red and blue curves respectively).

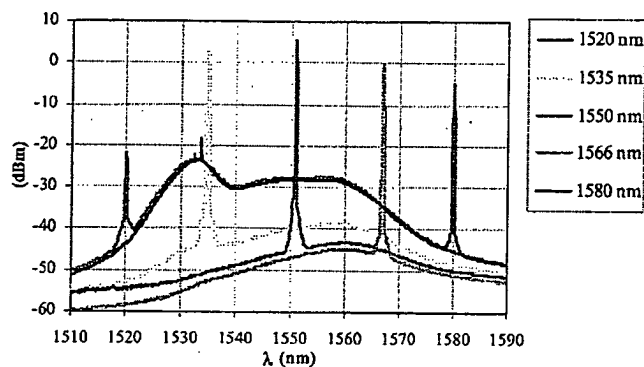


Fig. 8. Few typical spectra of the tunable Mach-Zehnder fiber laser obtained for five different adjustments of the grating orientation.

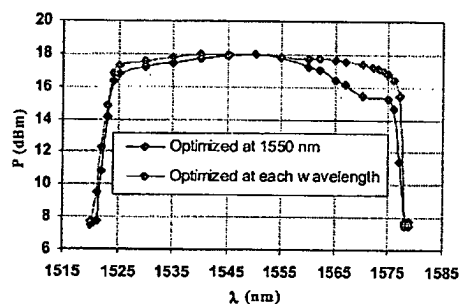


Fig. 9. Output power versus laser wavelength. The red curve was obtained by optimizing the output power with the polarization controller at each wavelength, whereas the output power was optimized only at 1550 nm for the blue curve.

These last results demonstrate, for the first time to our knowledge, that coherent combining of lasers is compatible with wavelength tuning. The technique represents an alternative method making a widely tunable fiber laser source of high power.

##### 5. N-arm interferometer resonator

We have also investigated the scaling of the method, for the combining of several elementary fiber lasers, only using standard 50/50 couplers. In a first step, we have successfully demonstrated the coherent combining of four fiber lasers. The experimental set-up, shown in figure 10, is a Mach-Zehnder tree architecture in which the coherent combining is achieved with 50/50 couplers in a cascading arrangement. Each EDFA is core pumped by a pigtailed laser diode emitting at 980nm with a power up to 100mW. One input port of the coupler  $C_3$  is cleaved in order to achieve the output coupler of the laser with a reflectivity of 4%. The end mirror of the laser is realized by splicing a chirped fiber Bragg grating with a high reflectivity ( $\geq 98\%$ ) at 1550 and 2nm bandwidth. In contrast, all the other coupler's input ports were angle cleaved to avoid any reflection in the laser resonator.

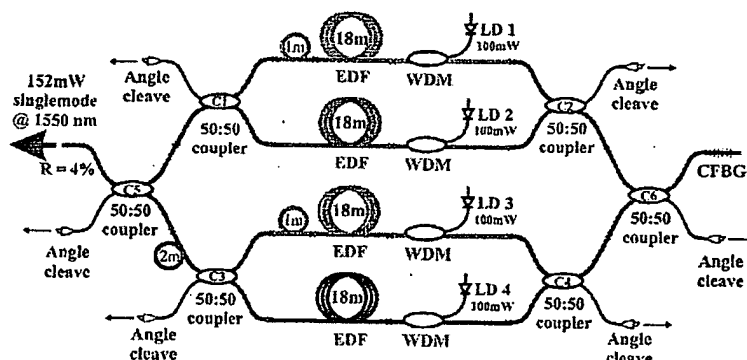


Fig. 10. Experimental set-up of the 4-arm fiber laser (4AFL).

We have measured the conversion efficiency of the 4-arm fiber laser (4AFL) to be compared with those obtained with the MZFL and an individual fiber laser (IFL). Figure 3 shows that the 4AFL threshold ( $\text{Thr}$ ) was twice the MZFL one. In each arm of the interferometric laser, the population inversion occurs at the same pumping level as in the IFL. The 4AFL, the MZFL and the IFL had almost the same slope efficiency ( $\eta_L$ ) of 44%. This means that the combining efficiency was maximum which was confirmed by the very low power leakage measured on the angle cleave output ( $<1\text{mW}$ ). At the highest pumping level of  $4 \times 100\text{mW}$ , the 4AFL output power reached  $152\text{mW}$ , almost four times the output power of an IFL ( $40\text{mW}$ ).

Finally, we theoretically investigated the resonator critical parameters in order to efficiently combine a high number of lasers in a single multi-arm cavity. The principle of coherent combining method is based on the use of an interferometric resonator configuration. The spectral response of such resonators determines the resonance frequencies of lowest losses which achieved a high efficient coherent combining. The multi-arm laser only amplifies these resonance frequencies. So, we have studied the spectral response of a N-arm interferometer resonator by using the circulating field theory [9-10]. In that way, one can estimate the intracavity losses and so the combining efficiency of the multi-interferometer resonator.

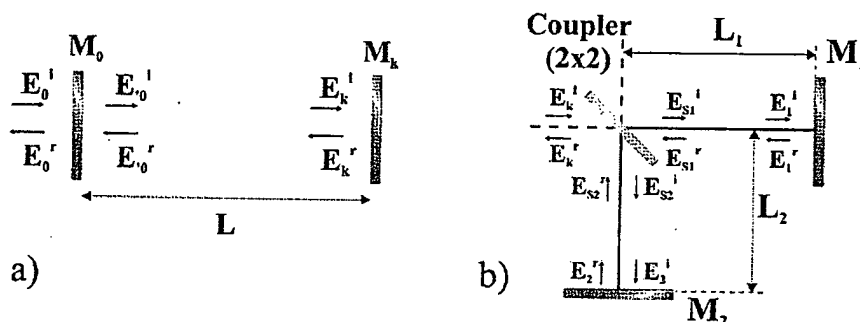


Fig. 11. Scheme and nomenclature of a) the Fabry-Perot resonator; b) the Michelson interferometer.

The well-known complex amplitude reflectivity  $r_{eq}$  of a Fabry-Perot cavity (see figure 11a) is given by:



$$r_{eq} = \frac{E_0^r}{E_0^i} = \frac{r_0 + r_k e^{\frac{j2\omega L}{c}}}{1 + r_0 r_k e^{\frac{j2\omega L}{c}}} \quad (1)$$

with the output coupler reflectivity  $r_0$  and the back mirror reflectivity  $r_k = \frac{E_k^r}{E_k^i}$ .

By replacing the back mirror reflectivity  $r_k$  of the Fabry-Perot resonator by the equivalent complex reflectivity of a N-arm interferometer  $r_{kN}$ , one can determine the spectral response of the N-arm interferometer resonator.

We first consider the case of the standard Michelson interferometer, which has a similar spectral behavior than the Mach-Zehnder device with two arms as depicted in Fig. 11b. All the circulating fields used in the next equations are defined on the Fig. 11. The circulating field expressions are:

$$E_{s1}^i = t_1 E_k^i; E_1^i = e^{\frac{j\omega L_1}{c}} E_{s1}^i; E_1^r = r_1 E_1^i; E_{s1}^r = e^{\frac{j\omega L_1}{c}} E_1^r \quad (2)$$

$$E_{s2}^i = r_1 E_k^i; E_2^i = e^{\frac{j\omega L_2}{c}} E_{s2}^i; E_2^r = r_1 E_2^i; E_{s2}^r = e^{\frac{j\omega L_2}{c}} E_2^r \quad (3)$$

$r_1$  and  $t_1$  are respectively the reflectivity and the transmission of the 2x2 coupler.

They lead to :

$$E_k^r = [t_1^2 r_1 e^{\frac{j2\omega L_1}{c}} + r_1^2 r_2 e^{\frac{j2\omega L_2}{c}}] E_k^i \quad (4)$$

We consider a balanced 2x2 coupler such that  $r_1^2 = t_1^2 = \frac{1}{2}$ . Then, the complex reflectivity of the interferometer device is:

$$r_{k2} = \frac{E_k^r}{E_k^i} = \frac{1}{2} [r_1 e^{\frac{j2\omega L_1}{c}} + r_2 e^{\frac{j2\omega L_2}{c}}] \quad (5)$$

We find the expression of the complex reflectivity  $r_{kN}$  of the N-arm interferometer by extrapolation:

$$r_{kN} = \frac{1}{N} \sum_{k=1}^N r_k e^{\frac{j2\omega L_k}{c}} \quad (6)$$

It has to be noted that the expression of  $r_{kN}$  does not depend on the position of the 2x2 couplers or of the fiber couplers in the tree architecture of the N-arm interferometer resonator. So, the whole 2x2 couplers of the experimental 4-arm fiber laser previously described could be replaced by a single 4x4 coupler operating in the same way [2].

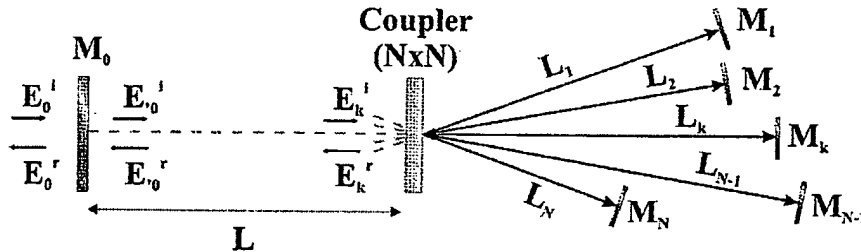


Fig. 12. Scheme and nomenclature of the N-arm interferometer resonator.

Finally, we replace the end mirror  $M_k$  of the Fabry-Perot cavity by the N-arm interferometer (Fig. 12). Then, the equivalent complex reflectivity of the N-arm interferometer resonator  $r_{eqN}$  is:

$$r_{eqN} = \frac{E_o^r}{E_o^i} = \frac{r_o + r_{kN} e^{\frac{j2\omega L}{c}}}{1 + r_o r_{kN} e^{\frac{j2\omega L}{c}}} \quad (7)$$

and the intensity spectral response of the N-arm interferometer resonator is:  $R_{eqN} = \|r_{eqN}\|^2$ .

We numerically have investigated the spectral response of the multi-interferometer resonator. In order to control the minimal path length difference between all the arms of the resonator, they had a constant average length difference  $\Delta L$ . A random length deviation  $\delta l_i$  was added such that the length  $L_i$  of the elementary resonator  $i$  was defined as:  $L_i = L_c + i\Delta L + \delta l_i$ .  $L_c$  was the minimal length of the elementary resonators.  $\delta l_i$  was chosen to take into account the difficulty to cut a long fiber at a precise length. The next calculus was obtained with the following data:  $L_c = 20m$ ;  $r_o^2 = 0.04$ ;  $-\Delta L/10 \leq \delta l_i \leq \Delta L/10$ ;  $\Delta\lambda = 1nm$ , spectrum bandwidth centered on  $\lambda_0 = 1550nm$ .

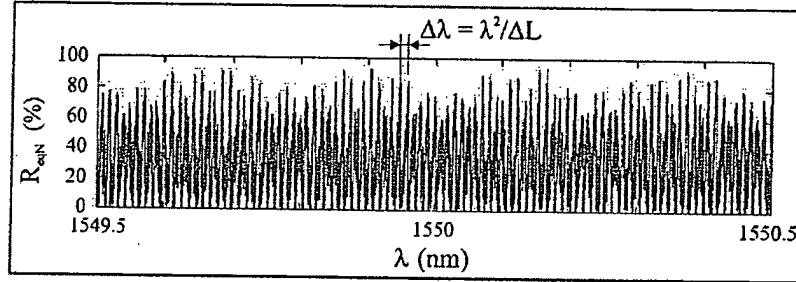


Fig. 13 Calculated intensity spectral response of a 20-arm interferometer resonator with an average length difference  $\Delta L = 10cm$ .

An example of the  $R_{eqN}$  function plotted Fig. 13 is calculated by considering an interferometer resonator of 20 arms and  $\Delta L = 10cm$ . One observes a predominant modulation of the spectrum due to the constant average length difference  $\Delta L$ . The large number of modulations in the spectrum bandwidth must ensure both high combining efficiency and output power stability as previously discussed in the Michelson or Mach-Zehnder fiber laser. The intracavity losses are closely connected to the intensity reflectivity of the resonator spectral response. Indeed, only the resonance frequencies corresponding to the highest value of  $R_{eqN}$  are amplified in the multi-interferometer laser. The numerical results also show that the number  $N$  of arms has no influence on the combining efficiency of the multi-interferometer resonator. Figure 14 describes the evolution of the highest reflectivity  $\max(R_{eqN})$  in the spectrum as a function of the number of arms.  $\max(R_{eqN})$  has small fluctuations around an high average value of  $\sim 94\%$  for  $\Delta L = 10cm$ . However, this average reflectivity decreases with the minimal arm length difference  $\Delta L$  as shown figure 15 as and when the number of modulations due to  $\Delta L$  decreases in the spectrum bandwidth. The intracavity losses are complementary to  $\max(R_{eqN})$ . The numerical results of the figure 15 show that these losses become critical only for a very small value of  $\Delta L$  which is not realistic experimentally.

These last experimental and numerical results demonstrate that the coherent coupling method is compatible with the combining of a large number of lasers without loss of efficiency.

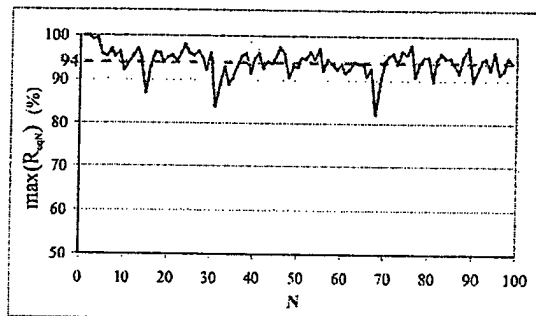


Fig. 14. Calculated evolution of the highest reflectivity  $\max(R_{eqN})$  of the spectral response, as function of the number of arms  $N$  for  $\Delta L = 10$  cm.

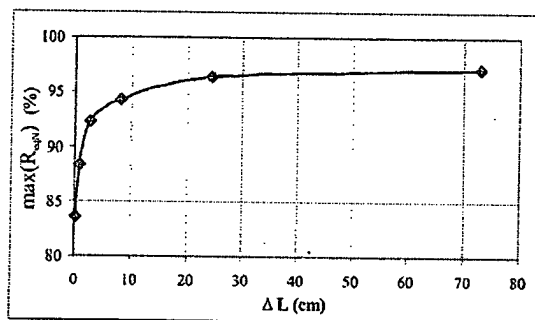


Fig. 15. Calculated evolution of the highest reflectivity  $\max(R_{eqN})$  of the spectral response, as function of the average arm length difference  $\Delta L$ .

## 6. Conclusion

We have experimentally demonstrated high efficiency coherent combining of 2 and then 4 fiber lasers. We have determined the condition minimizing the output power fluctuations in spite of the interferometric configuration: the arm length difference has to be large enough to provide spectrum modulations of period smaller than the laser-spectral bandwidth. We have also experimentally shown that the combining method can be applied to tunable laser sources by tuning a Mach-Zehnder Fiber Laser on a wide spectral range of 60nm covering the whole gain bandwidth of erbium doped fibers. Finally, a theoretical study confirms that the combining method can be successfully scaled and applied to a large number of lasers without decreasing the combining efficiency.